Article

Purification of Textile Effluents Containing C.I. Acid Violet 1: Adsorptive Removal versus Hydrogen Peroxide and Peracetic Acid Based Advanced Oxidation

Monika Wawrzkiewicz [1],*[ID]**, Urszula Kotowska** [2] **and Aneta Sokół** [2][ID]

[1] Department of Inorganic Chemistry, Institute of Chemical Sciences, Faculty of Chemistry, Maria Curie-Sklodowska University in Lublin, M. Curie-Sklodowska Sq. 3, 20-031 Lublin, Poland

[2] Department of Analytical and Inorganic Chemistry, Faculty of Chemistry, University of Bialystok, Ciolkowskiego 1K St., 15-245 Bialystok, Poland; ukrajew@uwb.edu.pl (U.K.); a.sokol@uwb.edu.pl (A.S.)

* Correspondence: m.wawrzkiewicz@poczta.umcs.lublin.pl; Tel.: +48-81-537-57-38

Abstract: Textile effluent containing azo dyes such as C.I. Acid Violet 1 (AV1) can be degraded to toxic aromatic amines in the environment. Thus, there is a legitimate need to treat such effluents before they are discharged to surface waters. Two methods were proposed to remove AV1 from aqueous solutions: adsorption and advanced oxidation processes (AOPs). The sorption capacity of the strongly basic anion exchanger Purolite A520E of the polystyrene matrix determined from the Langmuir isotherm model was found to be 835 mg/g, while that of Lewatit S5428 of the polyacrylamide matrix Freundlich model seems to be more appropriate for describing the experimental data. The pseudo-second-order kinetic model and external diffusion are the rate limiting steps of adsorption. The removal efficiency of AV1 by the anion exchangers was higher than 99% after 40 min of phase contact time. AOPs involved the usage of hydrogen peroxide and peracetic acid (PAA) as oxidizing agents, while Fe^{2+} and simulated sunlight were used as oxidizing activators. AV1 oxidation followed the pseudo-first-order kinetics, and the systems with the highest values of the rate constants turned out to be those in which Fe^{2+} was present. The efficiency of oxidation measured by the degree of decolorization in the systems with Fe^{2+} was higher than 99% after 10–60 min. AV1 mineralization was slower, but after 120 min of oxidation it was higher than 98% in the H_2O_2/Fe^{2+}, PAA/Fe^{2+} and PAA/Fe^{2+}/sunlight systems.

Keywords: dye; anion exchanger; textile effluents; adsorption; advanced oxidation; hydrogen peroxide; peracetic acid

1. Introduction

Synthetic dyes are widely used in various industries, including the production of textiles, food, plastic, cosmetics and paper. According to current data, more than 100,000 dyes are known, and their annual production has reached 700,000 tons [1]. The consumption of dyes in the textile industry around the world exceeds 10,000 tons per year, of which about 1% is discharged into the aquatic environment [2].

Dyes are characterized by intense color, even when their concentrations are small [3–5]. They can affect the photosynthetic activity of aquatic plants due to the reduced penetration of light. Dyes also show toxicity for some aquatic organisms, and their carcinogenic, mutagenic or teratogenic effects have been proved in relation to some microorganisms and fish species [6,7]. It was estimated that LD50 (lethal dose, 50%) values greater than 2×10^3 mg/kg were exhibited by 90% of the 4000 dyes tested. The highest toxicity was found for basic and diazo direct dyes [8]. Dyes may adversely affect human health, causing dysfunction of the kidneys, reproductive system, liver, brain and central nervous system [9]. Particularly dangerous is the introduction of azo dyes into the environment, which are broken down to toxic amines [8]. A number of chemical (including photochemical and

electrochemical), biological and physical methods are used to remove dyes from polluted waters [10–18].

The biological methods used to remove dyes include bioremediation using bacteria, algae, fungi and systems of cooperating plants and microbes, phytoremediation and the use of plant parts and enzymes. Biological methods are cheap and environmentally friendly, while their main limitation is the insufficient efficiency of removal in relation to many dyes.

Physical treatment includes membrane filtration, electrokinetic coagulation and sorption methods. The main advantage of the first two methods is the high efficiency of decolorization, while the disadvantage is the formation of large amounts of concentrated sludge production [16].

Adsorption is one of the most effective wastewater treatment processes [17]. Many textile companies use commercial activated carbon to remove dyes from wastewater. Currently, research is focused on the use of alternative materials for commercial activated carbon, which is a very effective sorbent, but its use is associated with high costs [10,18].

One of the directions of research is the search for low-cost adsorbents of natural origin or obtained from industrial or agricultural solid waste [19–21]. Various unconventional adsorbents, including clay, wheat bran fly ash, walnut husk, microalga *Spirulina platensis*, *Cucumis sativus*, rice straw, crop residues, maize cob, barley hull, nanomaterials and *Salxi babylonic* leaf powder, have been used to remove dyes from aqueous solutions [19–21]. The disadvantages of this type of adsorption material are its very low capacity for dyes and low mechanical and chemical strength, as well as physicochemical properties that depend, e.g., on the region of occurrence of a given material, which make it difficult to compare their effectiveness.

An alternative to this type of material may be ion exchange resins. They are characterized primarily by a very high sorption capacity towards dyes and excellent chemical stability and mechanical strength. The wide range of materials of this type available on the market allows them to be used to remove dyes of anionic and cationic nature. In addition, high resistance to pressure changes enables their use in the column system. The disadvantage of their use is the cost of building an industrial-scale plant. Not only cation exchangers but also anion exchangers with polystyrene, polyacrylic and phenol-formaldehyde matrices as well as different basicities of functional groups (i.e., weakly, intermediate and strongly basic) such as Lewatit MonoPlus MP62, Lewatit MonoPlus MP64, Purolite A847, Amberlite IRA67, Amberlite IRA 478, Amberlite IRA 458, Amberlite IRA958, Amberlyst A21, Amberlyst A23 or Amberlyst A24 have been used to remove acid (e.g., C.I. Acid Orange 7, C.I. Acid Red 18, C.I. Acid Blue 249, C.I. Acid Green 16, C.I. Acid Violet 1), direct (e.g., C.I. Direct Blue 71, C.I. Direct Red 75, C.I. Direct Yellow 50) and reactive (e.g., C.I. Reactive Black 5, C.I. Reactive Blue 21) dyes from model solutions and wastewater [22–31].

Chemical methods used for dyes in wastewater treatment mainly include advanced oxidation processes, most often using ozone, hydrogen peroxide and hydrogen peroxide in combination with Fe^{2+} salts (Fenton's reagent) [32–34]. Oxidation processes are usually highly effective in decolorizing solutions containing both azo dyes and dyes with different structures, also in the form of mixtures [35–38]. The main characteristics of AOPs are the in-situ production of highly reactive radicals capable of the degradation of organic chemicals. The most frequently produced radical is ˙OH, which has a high standard oxidizing potential and reacts non-selectively with compounds present in its environment. Oxidation can take place in a homogeneous or heterogeneous system. In the latter, the oxidation activator is a solid substance—most often TiO_2 and other transition metal oxides. In photochemical methods, ultraviolet or visible light is used as an oxidation-promoting agent. Light activation is combined with oxidation with ozone, H_2O_2 and the Fenton reaction and used in photocatalysis processes [39]. To increase the efficiency of oxidation processes, other physical factors such as electric current (electro-Fenton reaction), ultrasounds, microwaves, heat and ionizing radiation are also used [40].

Relatively recently, inorganic peracids in the form of salts—i.e., peroxymonosulfates (PMS) and persulfates (PS)—as well as organic peracids, mainly peracetic acid (PAA), have

been used as oxidants in AOPs processes [41–43]. Oxidation in these processes takes place through the action of radicals formed in the solution, which besides ˙OH are $SO_4^{˙-}$ or $CH_3COO˙$ [41]. Oxidation processes under the influence of PAA, which, as a non-toxic and environmentally friendly compound, is widely used in practice to disinfect surfaces intended for contact with food, are particularly little studied [42]. Similar factors are used to activate PAA as in the case of H_2O_2. The most commonly used are Fe^{2+} ions (pseudo-Fenton system) and UV light [41]. Due to the method of synthesis, commercial preparations of this compound exist in the form of an equilibrium mixture of PAA and H_2O_2.

　　　The main advantage of AOPs is that the removed contaminants are degraded into simpler compounds. In most cases, organic compounds are completely mineralized and converted to carbon dioxide, water and inorganic salts [44].

　　　The aim of this study was to compare the efficiency of AV1 (C.I. Acid Violet 1) dye removal by the adsorption technique using anion exchange resins and by an advanced oxidation process using hydrogen peroxide and peracetic acid. Parameters influencing the adsorption of AV1 on the anion exchangers such as initial dye concentration, phase contact time and presence of additives (Na_2SO_4, CH_3COOH, anionic and non-ionic surfactants) were investigated by determining kinetic and equilibrium parameters. Regeneration efficiency was also evaluated. The course of AV1 oxidation in seven different oxidation systems based on the use of hydrogen peroxide (H_2O_2 alone, H_2O_2/solar light, H_2O_2/Fe^{2+}) and peracetic acid (PAA alone, PAA/solar light, PAA/Fe^{2+}, PAA/Fe^{2+}/solar light) was determined. The influence of the oxidant concentration on the course of the processes was investigated and kinetic studies were performed. The efficiency of the oxidation processes was determined both on the basis of changes in absorbance in the maximum of absorption (decolorization), as well as on the basis of changes in chemical oxygen demand (COD), which allowed for the evaluation of mineralization.

2. Materials and Methods

2.1. Materials

　　　C.I. Acid Violet 1 (C.I. 17025) is a single azo-type dye (Figure 1). It was obtained from Boruta-Kolor S.A. (Zgierz, Poland) and was used without additional purification.
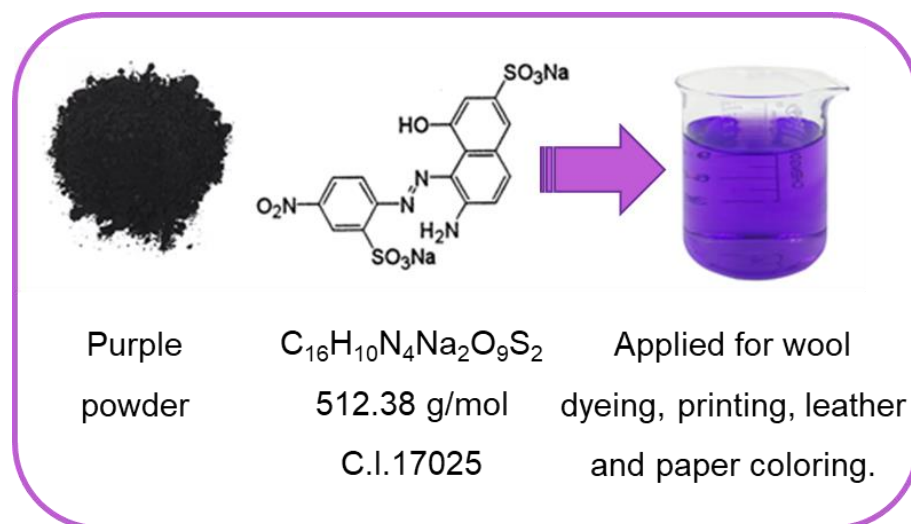
Figure 1. C.I. Acid Violet 1 properties.

　　　Two resins of the anion exchange type were applied in the adsorption test. Both resins are the strongly basic anion exchangers of a macroporous structure but with a different matrix composition. The anion exchangers' properties are presented in Table 1.

Table 1. Anion exchange resins properties [45,46].

Properties	Lewatit S5428	Purolite A520E
Functional groups	Quaternary ammonium, type 1	
Ionic form as shipped	Cl^-	
Matrix	Crosslinked polyacrylamide	Crosslinked polystyrene
Structure	macroporous	
Total capacity (eq/L)	0.85	0.9
Water retention (%)	63–68	50–56
Mean bead size (mm)	0.4–1.6	0.3–1.2
Max. operating temperature (°C)	80	100
Operating pH range	0–12	0–12
Appearance	White, opaque	Cream, opaque
Manufacturer	Lenntech, The Neterhlands	Purolite, United States

Two surfactants—anionic sodium dodecyl sulfate (SDS) and non-ionic 2-[4-(2,4,4-trimethylpentan-2-yl)phenoxy]ethanol Triton X-100 (TX100) of laboratory grade—were obtained from Sigma-Aldrich (Germany). Sodium sulfate, sodium chloride, acetic acid, hydrochloric acid, sodium hydroxide and methanol of analytical grade were purchased from Avantor Performance Materials Poland S.A. (Poland). Acetic acid, hydrogen peroxide, sulfuric(VI) acid, iron(II) sulfate(VI) heptahydrate and sodium thiosulfate of analytical grade were purchased from Chempur (Poland). COD cuvette tests—ISO 15705, 0–150 mg/L O_2—were obtained from Hach Lange (Germany).

2.2. Methods

2.2.1. Adsorption and Desorption Tests

The adsorption studies were carried out at room temperature by the batch technique. This involves shaking the known amount of the anion exchanger (0.5 g) with an aqueous solution of predetermined volume (50 mL) and initial concentration during a defined time (from 1 to 240 min (kinetic tests) or 24 h (isothem studies)) using an Erlenmeyer flask. After shaking on a mechanical shaker (Elpin Plus, Lubawa, Poland) at an amplitude of 7 and 180 rpm, the resins were separated by filtration, and the concentration of the dye was measured using a UV–VIS spectrophotometer Cary 60 (Agilent Technologies, Santa Clara, CA, USA) by measuring absorbance at λ_{max} = 552 nm.

The initial AV1 concentrations used to evaluate the isotherm and kinetic data ranged from 1000 to 10,000 mg/L and from 100 to 500 mg/L, respectively. The initial pH of the solutions was ~4.85. Effects of auxiliaries such as electrolytes, acid and surfactants on the AV1 sorption by the anion exchangers was investigated in the systems with the following composition: 500 mg/L AV1 + 5–25 g/L Na_2SO_4, 500 mg/L AV1 + 0.25–1 g/L CH_3COOH, 500 mg/L AV1 + 0.1–0.25 g/L SDS and 500 mg/L AV1 + 0.1–0.25 g/L TX100 during a sorption time t of 15 min. The amounts of AV1 adsorbed by the S5428 and A520E anion exchangers at equilibrium (q_e) and at time t (q_t) as well as removal efficiency (RE) were calculated from the equations

$$q_e = \frac{(C_0 - C_e)}{m} \cdot V \tag{1}$$

$$q_t = \frac{(C_0 - C_t)}{m} \cdot V \tag{2}$$

$$RE = \frac{(C_0 - C_t)}{C_0} \cdot 100\% \tag{3}$$

where C_0, C_e and C_t (mg/L) show AV1 concentrations in the solution before adsorption, at equilibrium and after sorption time t, respectively; V (L) is the volume of AV1 solution; and m (g) is the mass of S5428 and A520E.

Three isotherm models were applied in order to determine the adsorption equilibrium parameters for AV1 retention on the strongly basic anion exchange resins: the Langmuir, the Freundlich and the Temkin [47–51]. Kinetic data were modeled using the most popular

kinetic equation; i.e., the pseudo-first order by Lagergren, the pseudo-second order by Ho and the intraparticle diffusion by Weber and Morris [47–51]. Table 2 summarizes the above-mentioned equilibrium and kinetic models.

Table 2. Isotherm and kinetic models used for the description of adsorption equilibrium systems.

Isotherm	Equation No.	Linear Forms	Plot
Langmuir	(4)	$\frac{C_e}{q_e} = \frac{1}{Q_0 k_L} + \frac{C_e}{Q_0}$	C_e/q_e vs. C_e
Freundlich	(5)	$\log q_e = \log k_F + \frac{1}{n} \log C_e$	$\log q_e$ vs. $\log C_e$
Temkin	(6)	$q_e = \left(\frac{RT}{b_T}\right) \ln A + \left(\frac{RT}{b_T}\right) \ln C_e$	q_e vs. $\ln C_e$
Pseudo-first order (PFO)	(7)	$\log(q_e - q_t) = \log(q_t) - \frac{k_1}{2.303} t$	$\log(q_e - q_t)$ vs. t
Pseudo-second order (PSO)	(8)	$\frac{t}{q_t} = \frac{1}{k_2 q_e^2} + \frac{1}{q_e} t$	t/q_t vs. t
Intraparticle diffusion (IPD)	(9)	$q_t = k_i t^{1/2}$	q_t vs. $t^{0.5}$

where q_e (mg/g)—amount of AV1 adsorbed at equilibrium per unit mass of A520E and S5428, q_t (mg/g)—amount of AV1 adsorbed at time t per unit mass of A520E and S5428, C_e (mg/L)—equilibrium concentration of AV1 in solution, Q_0 (mg/g)—monolayer adsorption capacity, k_L (L/mg)—the Langmuir constant (related to the free energy of adsorption), K_F (mg$^{1-1/n}$ L$^{1/n}$/g) and n—the Freundlich constants related to adsorption capability and adsorption intensity, respectively, R (8.314 J/mol K)—gas constant, T (K)—temperature, A (L/g) and b_T (J/mol)—the Temkin constants, k_1 (1/min) and k_2 (g/mg min)—rate constants of sorption determined from PFO and PSO equations, respectively, k_i (mg/g min$^{0.5}$)—intraparticle diffusion rate constant.

Desorption studies were performed using samples of anion exchangers (0.5 g) uploaded with AV1, (q_e = 50 mg/g). The resin beads were shaken for 3 h with 50 mL of regenerants such as 1 M NaCl, 1 M NaOH, 1 M HCl, 1 M NaCl + 50% *v/v* CH$_3$OH, 1 M NaOH + 50% *v/v* CH$_3$OH and 1 M HCl + 50% *v/v* CH$_3$OH. Three cycles of sorption and desorption were performed. The amount of AV1 desorbed form the anion exchanger phase was evaluated using UV-vis measurements and calculated by mass balance as a desorption percentage using the following formula:

$$D = \frac{m_{des}}{m_{ads}} \cdot 100\% \tag{10}$$

where m_{des} is the mass of AV1 desorbed (mg) and m_{ads} is the mass of AV1 adsorbed (mg).

The adsorption and desorption experiments were carried out in triplicate, and the mean value is presented. The standard deviation did not exceed 5%.

2.2.2. Advanced Oxidation Processes

Peracetic acid solution was prepared according to the following procedure: 10 mL of 99.5% acetic acid and 0.94 mL of 95% sulfuric (VI) acid were added to the ground glass bottle. Then, 10 mL of 30% hydrogen peroxide solution was gradually added to the mixture. The bottle was closed with a stopper, placed in an ice bath and mixed by a magnetic stirrer for 90 min. Then, the prepared peracetic acid solution was stored tightly closed in a refrigerator at 4 °C. It was found that directly after mixing the reagents, the PAA concentration was 9%, which reached the maximum value of 16% after two days. PAA stored at 4 °C exhibited stability for about one month.

Oxidation experiments were conducted in 100 mL glass beakers with magnetic stirring at room temperature. Solutions of AV1 at a concentration of 100 mg/L were mixed with appropriate volumes of H$_2$O$_2$ or peracetic acid. After a certain period of time, the reaction was stopped by the addition of 2 mL of 20% solution of sodium thiosulfate, and the concentration of the dye was measured using a UV–VIS spectrophotometer. In the same manner, the oxidation experiments assisted by sunlight and the presence of Fe(II) ions were performed. In the case of the light-assisted oxidation process, a prepared mixture of studied compounds with the addition of appropriate portions of H$_2$O$_2$ or peracetic acid was subjected to the irradiation in the solar light simulator (SUNTEST CPS+, ATLAS, Champaign, IL, USA) emitting radiation in the range of 300–800 nm. The temperature in the simulator was maintained at 30 °C. To check the influence of Vis light on the kinetics of AV1 degradation, the lamp worked in one mode set at 750 W/m^2 for all experiments.

3. Results

3.1. Adsorption Studies

3.1.1. Isotherm Experiments

The interactions of dye molecules with the adsorbent can be considered using equilibrium sorption data. Adsorption isotherms explain how pollutants such as azo dyes may be bound by the functional group present on the surface or inside the adsorbent. The Langmuir model considers that the pollutant (i.e., dye) retention occurred on the homogeneous surface of the adsorbent and the monolayer is formed without chemical interactions or bond formation. Freundlich proposed a different isotherm model that assumes adsorption on a heterogonous surface with the formation of a multilayer. The Temkin isotherm states that due to adsorbent–adsorbate interactions, after ignoring very low and high values of concentrations, the adsorption heat of all molecules in the layer will decrease linearly with coverage. The above-mentioned isotherm constants calculated from the corresponding plots are listed in Table 3.

Table 3. The Langmuir, Freundlich and Temkin isotherm parameters for AV1 adsorption on the polystyrene and polyacrylamide resins.

Isotherm	Parameters	
	Purolite A520E	**Lewatit S5428**
Langmuir		
Q_0 (mg/g)	835.8	9867.9
k_L (L/mg)	0.718	0.019
R^2	0.999	0.435
Freundlich		
k_F (mg$^{1-1/n}$ L$^{1/n}$/g)	305.3	184.5
$1/n$	0.238	0.967
R^2	0.834	0.997
Temkin		
A (L/g)	75.68	1.69
b_T (J/mol)	27.82	6.98
R^2	0.881	0.927

As can be seen in Table 3 and Figure 2, the Langmuir isotherm described the adsorption of AV1 on the polystyrene anion exchange resin A520E with the determination coefficient R^2 value of 0.999. The Q_0 and k_L values obtained from the plot C_e/q_e vs. C_e were 835.8 mg/g and 0.718, respectively. The observable plateau in Figure 2a indicates a good fit of the experimental data in AV1-A520E system and suggests that the AV1 adsorption onto the polystyrene anion exchange resin A520E occurred with the formation of a monolayer. However, the low value of the k_L coefficient confirmed the weak forces between the dye anions and the A520E resin. The Freundlich isotherm parameters k_F and $1/n$ were equal to 305.3 mg$^{1-1/n}$ L$^{1/n}$/g and 0.238, respectively. The $1/n$ value was lower than unity, which indicates the favorable adsorption of AV1 by the A520E resin. Taking into account the b_T value calculated from the Temkin isotherm model, equal to 27.82 J/mol, it can be stated that the mechanism involved in AV1 uptake by A520E is physical adsorption (the bonding energy was below 8 kJ/mol); however, R^2 was found to be 0.881. Analyzing Figure 2b concerning AV1 adsorption on the polyacrylamide anion exchanger S5428, a linear relationship between q_e and C_e was observed. The Freundlich isotherm model provided the best fitting to experimental data compared to the Langmuir and Temkin models as the determination coefficient R^2 was 0.997. The values of k_F and $1/n$ were equal to 184.5 mg$^{1-1/n}$ L$^{1/n}$/g and 0.967.
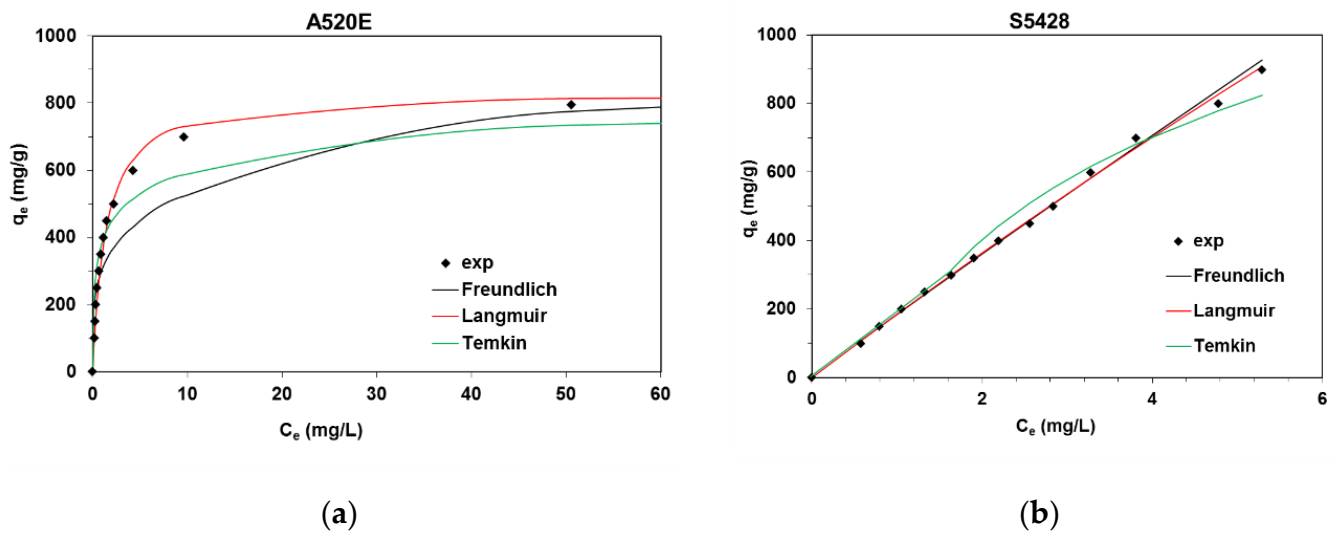
Figure 2. Linear fitting of the equilibrium sorption data to the Langmuir, Freundlich and Temkin isotherm models in (**a**) AV1-A520E and (**b**) AV1-S5428 systems.

The performed studies confirm the very good adsorption parameters of the applied anion exchangers in comparison with literature data. The divinylbenzene copolymer with glycidyl methacrylate of trietylenetetramine functional groups (DVB-co-GMA-TETA) exhibited a sorption capacity for AV1 of 216.3 mg/g, while for A520E, it was 835.8 mg/g. The experimental results described in [31] confirm that the equilibrium data can be successfully described by the Freundlich adsorption model. The adsorbent prepared from waste red mud during the processing of bauxite ore in the aluminum factory in India was able to remove AV1 at the amount of 1.4 mg/g [52].

To summarize the above considerations, it can be stated that two mechanism of dye binding by anion exchangers may be involved: these are ion exchange and physical adsorption. Ion exchange concerns the electrostatic interaction between functional groups of the anion exchangers with a positive charge (i.e., quaternary ammonium) and sulfone groups of a dye anion. Physical adsorption such as π–π interactions between the matrix of the anion exchangers and aromatic rings present in the dye molecules also occurred. The acrylamide matrix of S5428 resin is more elastic and hydrophilic than the styrene-based copolymer of A520E, which is also very important during the retention of large organic species (of high molecular weight) such as dyes. The sorption of dye anions by an acrylamide matrix of S5428 with a more aliphatic skeletal structure enables van der Waals attraction between the resin matrix and the hydrocarbon structure of dye anions. The presence of the donor oxygen atom of the carbonyl group in the matrix of S5428 promotes interactions with protonated -NH_2 and -OH groups in the dye molecules.

3.1.2. Kinetic Experiments

Very important factors influencing the efficiency of AV1 uptake are the phase contact time between the adsorbent and adsorbate and initial concentration of dye in the solution, as well as the agitation speed. Figure 3a–f shows the impact of the above-mentioned parameters on AV1 sorption on A520E and S5428 and the fitting of experimental data to the three kinetic models: pseudo-first order (PFO), pseudo-second order (PSO) and intraparticle diffusion (IPD). The course of the experimental points on both resins was very similar, as shown in Figure 3a,b. The state of equilibrium in the AV1-A520E and AV1-S5428 systems was observed after 40 min of phase contact time, regardless of the initial AV1 concentration in the system.
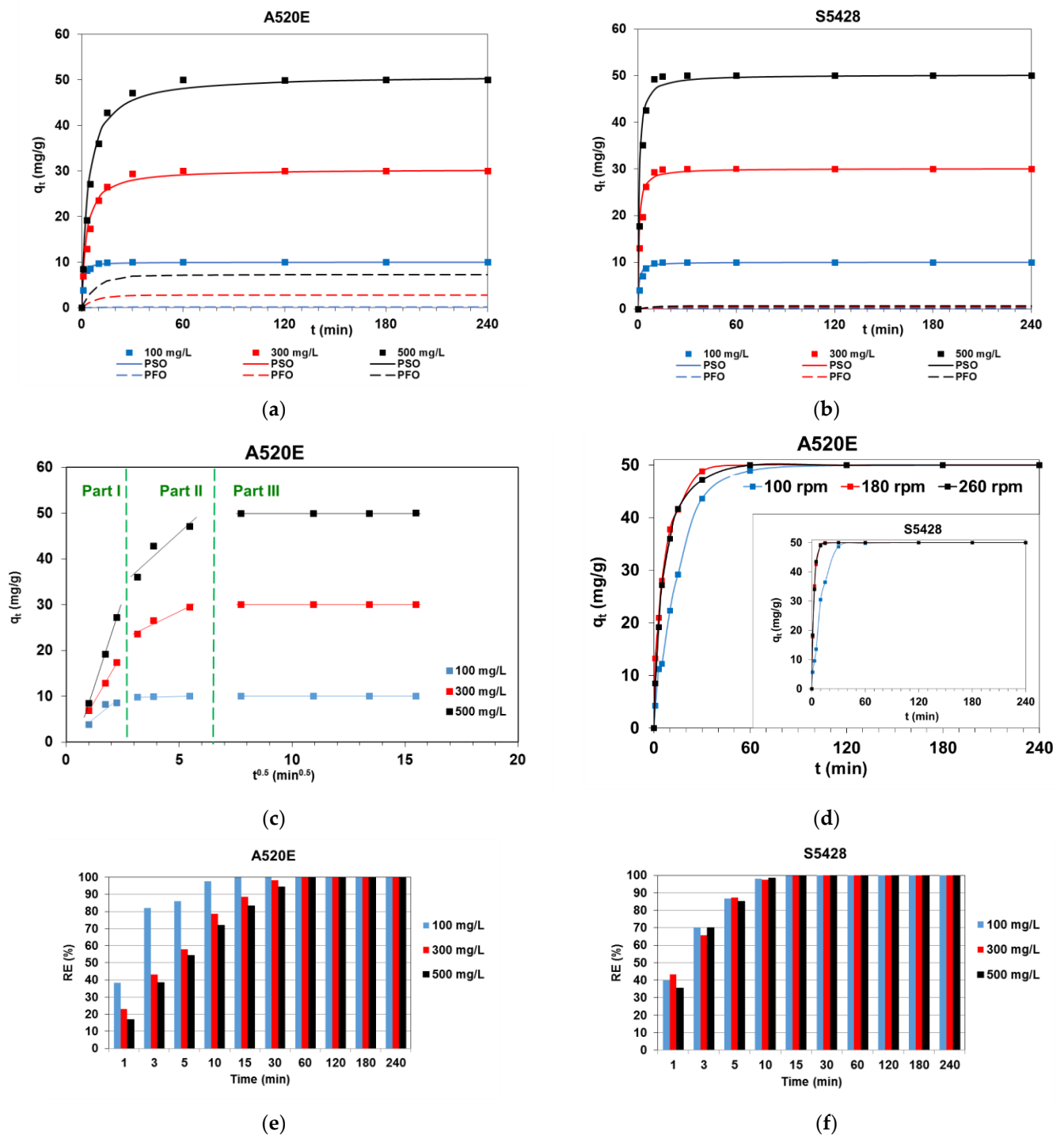
Figure 3. Kinetic plot in AV1-A520E and S5428 systems. Impact of phase contact time and initial dye concentration on the dye uptake as well as fitting lines to PFO and PSO models using (**a**) A520E and (**b**) S5428; (**c**) intraparticle diffusion plot for AV1-A520E system; (**d**) agitation speed impact on AV1 uptake (C_0 = 500 mg/L) by A520E and S5428; removal efficiency vs. time in 100-500 mg/L AV1 solutions using (**e**) A520E and (**f**) S5428.

The extremely short adsorption time of acid-type dyes on anion exchangers of various types necessary to reach equilibrium has been described in many papers [1–4]. For example, it is worth mentioning the removal of C.I. Acid Red 18 on the phenol-formaldehyde anion exchanger Amberlyst A23, C.I. Acid Green 16 on the polystyrene anion exchanger Lewatit S6368 [53–55].

Table 4 presents the calculated kinetic parameters during 100–500 mg/L AV1 adsorption on both resins. The non-linearity of the log ($q_e - q_t$) vs. *t* plots of the PFO model and the comparison of the sorption capacities determined from this model with the experimental data confirmed by the low values of R^2 allow us to conclude that it cannot be applied to description of kinetic data in the AV1–anion exchanger system. The PSO kinetic equation describes the experimental data with the highest R^2 values at 0.999. The values of the sorption capacities q_e determined from the PSO model are close to the experimental values ($q_{e,exp}$), both in the AV1–AE20E and AV1–S5428 systems. The q_e values calculated from the PSO model were equal to 10.02, 30.40 and 50.90 mg/g for A520E resin and 10.02, 30.10 and 50.19 mg/g for S5428 resin in 100, 300 and 500 mg/L solutions, respectively. The pseudo-second order rate constants k_2 decreased from 0.181 to 0.005 g/mg min for A520E and from 0.161 to 0.029 g/mg min for S5428 with the increasing dye concentration from 100 to 500 mg/L, respectively.

Table 4. Kinetic parameters for AV1 sorption from 100–500 mg/L solutions on the polystyrene and polyacrylamide resins.

Model	Parameter	Initial Dye Concentration C_0 (mg/L)		
		100	300	500
		Purolite A520E		
PFO	q_e (mg/g)	0.380	6.40	16.60
	k_1 (1/min)	0.028	0.0502	0.0494
	R^2	0.449	0.733	0.835
PSO	q_e (mg/g)	10.02	30.40	50.90
	k_2 (g/mg min)	0.181	0.012	0.005
	R^2	0.999	0.999	0.999
IPD	k_{i1} (mg/g min$^{0.5}$)	3.99	8.44	15.09
	R^2_1	0.887	0.999	0.999
	k_{i2} (mg/g min$^{0.5}$)	0.078	2.42	4.45
	R^2_2	0.572	0.948	0.885
	k_{i3} (mg/g min$^{0.5}$)	0.00001	0.00009	0.004
	R^2_3	0.691	0.822	0.791
$q_{e,exp}$ (mg/g)		9.99	29.99	49.99
		Lewatit S5428		
PFO	q_e (mg/g)	1.38	2.94	1.6
	k_1 (1/min)	0.028	0.035	0.039
	R^2	0.421	0.463	0.504
PSO	q_e (mg/g)	10.02	30.10	50.19
	k_2 (g/mg min)	0.161	0.052	0.029
	R^2	0.999	0.999	0.999
IPD	k_{i1} (mg/g min$^{0.5}$)	4.33	7.21	14.32
	R^2_1	0.972	0.965	0.946
	k_{i2} (mg/g min$^{0.5}$)	1.21	3.59	6.43
	R^2_2	0.679	0.703	0.671
	k_{i3} (mg/g min$^{0.5}$)	0.00002	0.00005	0.00013
	R^2_3	0.721	0.935	0.896
$q_{e,exp}$ (mg/g)		9.99	29.99	49.99

According to the IPD model, if the plots q_t vs. $t^{0.5}$ give a multilinearity, the adsorption of dye molecules can be controlled by two or more processes. As presented in Figure 4c, the plots of q_t vs. $t^{0.5}$ are multimodal with three regions: external diffusion (part I), intraparticle diffusion (part II) and surface adsorption (part III). Based on the values of k_{i1}, k_{i2} and k_{i3} and the determination coefficients of each part of the plot, it can be stated that not intraparticle diffusion but external diffusion was involved in the AV1 adsorption on A520E and S5428 and can thus be considered as one of the rate-limiting steps of adsorption. For comparison, the sorption of AV1 (C_0 = 100 mg/L) on DVB-co-GMA-TETA followed intraparticle diffusion, and the rate constant was found to be 10.39 mg/g min$^{0.5}$ [31].
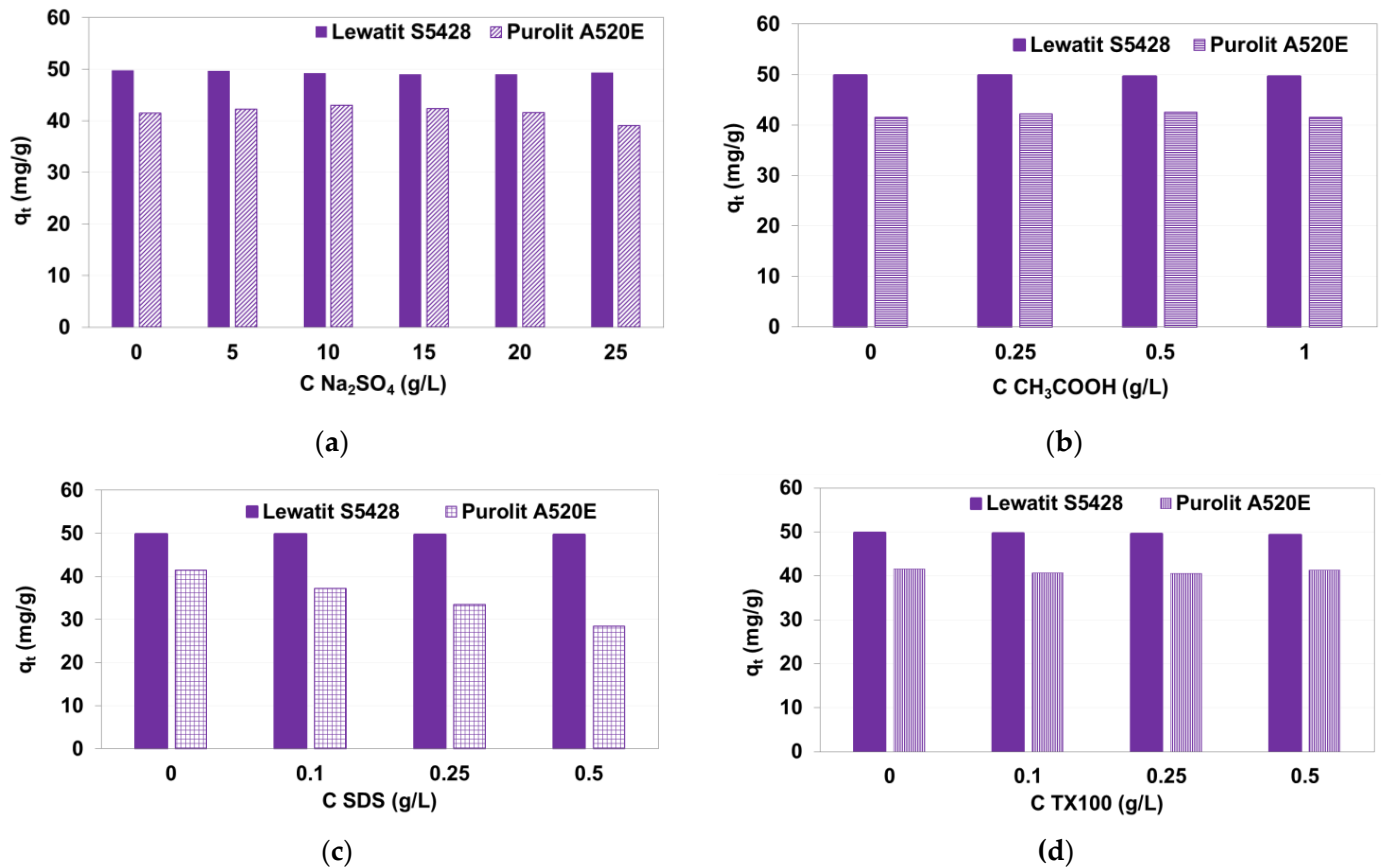
Figure 4. Influence of (**a**) Na_2SO_4, (**b**) CH_3COOH and (**c,d**) surfactants on AV1 uptake by A520E and S5428 anion exchangers.

The experimental parameter affecting the dye uptake by the resins is also the adsorption speed. It was observed in Figure 4d that the amount of AV1 adsorbed as a function of time increases with increasing shaking speed from 100 to 240 rpm. However, there was no significant difference between the q_t values calculated at 180 rpm and 240 rpm. Importantly, the shaking speed also has no significant effect on the time to reach equilibrium in the adsorption system.

The removal efficiency increased from 38.3% to 99.9%, from 23% to 99.9% and from 16.9% to 99.9% with increasing phase contact time in the systems containing 100, 300 and 500 mg/L of AV1 using A520E anion exchanger (Figure 4e). For S5428 resin, the values of *RE* were higher at the beginning of the dye sorption and equaled 39.9%, 43.3% and 35.5%, reaching values of 99.9% (Figure 4f) at equilibrium in 100–500 mg/L solutions, respectively. Adsorption of AV1 on a silica surface modified with 3-aminopropyl-triethoxysilane and N-2-(aminoethyl)-3-aminopropyltrimethoxysilane revealed that 52–99.6% and 79–99.8% of dye can be removed [53].

3.1.3. Impact of Auxiliaries on AV1 Sorption

The dye uptake by the anion exchangers can be influenced by additives such as electrolytes, acids or surfactants present in dyeing baths or effluents. In the current study, the AV1 removal was investigated from solutions with the following composition: 500 mg/L AV1 + 5–25 g/L Na2SO4, 500 mg/L AV1 + 0.25–1 g/L CH3COOH, 500 mg/L AV1 + 0.1–0.25 g/L SDS and 500 mg/L AV1 + 0.1–0.25 g/L TX100. Figure 4 presents the impact of the above-mentioned additives on the amount of AV adsorbed after 15 min of phase contact time.

The effect of salt, acid and surfactants in the established concentration range on the amount of retained dye (q_t) is more evident for its adsorption on the polystyrene anion exchanger A520E. A slight decrease in AV1 dye adsorption from 41.5 mg/g to 39.1 mg/g and from 41.5 mg/g to 28.4 mg/g was observed in dye baths containing sodium sulfate and sodium dodecyl sulfate—i.e., anionic surfactant—respectively. This can be explained by the competitive adsorption of the sulfate anions with a much smaller size compared to the anionic form of the AV1 dye. For the other systems, there was no noticeable change in the amount of AV1 adsorbed, which is very important from a practical point of view as these auxiliaries are present in both the dye baths and the wastewater.

3.1.4. Desorption Experiments

The desorption of AV1 from the anion exchangers was investigated using eluting agents such as 1 M HCl, 1 M NaOH and 1 M NaCl in aqueous and methanol solutions. As presented in Figure 5 the most effective regenerants were 1 M HCl + 50% *v/v* MeOH and 1 M NaCl + 50% *v/v* MeOH for both AV1 uploaded resins. The dye desorption values for S5428 during the first step of desorption were 70.5% and 86.7% using 1 M HCl + 50% *v/v* MeOH and 1 M NaCl + 50% *v/v* MeOH, respectively. During successive desorption cycles (1-3 cycles), a decrease in efficiency can be observed while keeping the sorption capacity almost constant. A lower desorption efficiency (59.7% and 73.3%) was observed for the A520E anion exchanger. Earlier performed studies were also in line with the present experiments and revealed that the methanol addition greatly improved desorption efficiency [22–31]. This is confirmed by the mixed mechanism of dye adsorption on anion exchangers, as described in Section 3.1.1, and the recognition of these adsorbents as selective for dye removal both from aqueous solutions and dyeing baths containing electrolytes and surfactants.
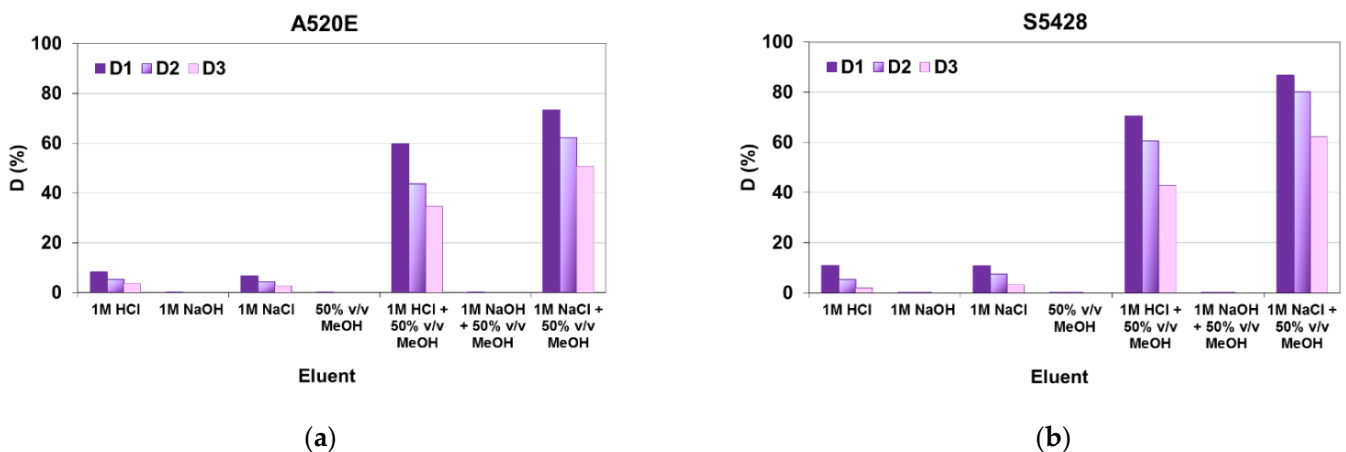
Figure 5. AV1 desorption from (**a**) A520E and (**b**) S5428 using different regenerant solutions.

3.2. Advanced Oxidation Processes

3.2.1. H$_2$O$_2$-Based Oxidation

Hydrogen peroxide is an environmentally friendly oxidant with a wide range of applications in various industries and in laboratory practice [56]. Breaking the O–O bond

in the H_2O_2 molecule occurs quite easily under the influence of various catalysts. The most commonly used catalysts are UV or sunlight and iron ions (Fenton reaction). In the presence of light, H_2O_2 decomposes into two hydroxyl radicals:

$$H_2O_2 + h\nu \rightarrow 2\ HO^\bullet \tag{11}$$

In the Fenton reaction, the production of $HO^\bullet$ occurs in an acidic environment in the presence of Fe^{2+}. The decomposition of H_2O_2 occurs due to the fact that Fe^{2+} ions play the role of an electron donor while oxidizing to Fe^{3+}:

$$Fe^{2+} + H_2O_2 \rightarrow Fe^{3+} + OH^- + HO^\bullet \tag{12}$$

An oxo-iron complex ($Fe^{IV}O^{2+}$) can be also formed in the Fenton process. It is a more selective and weaker oxidant than $HO^\bullet$ but has a longer lifetime [57]:

$$Fe^{2+} + H_2O \rightarrow Fe^{IV}O^{2+} + H_2O \tag{13}$$

Fe^{3+} formed in reaction (6) can also react with H_2O_2, but the rate of this reaction is low [58]:

$$Fe^{3+} + H_2O_2 \rightarrow Fe^{2+} + HO_2^\bullet + H^+ \tag{14}$$
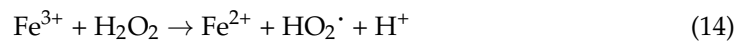
To study the process of dye removal during oxidation, the absorbance changes at absorption maximum were monitored and converted into the AV1 concentration by using calibration plots. Figure 6 shows the effect of H_2O_2 alone (Figure 6a) as well as H_2O_2 activated by simulated solar light (Figure 6b) and Fe^{2+} ions (Figure 6c).

(a)

(b)

(c)
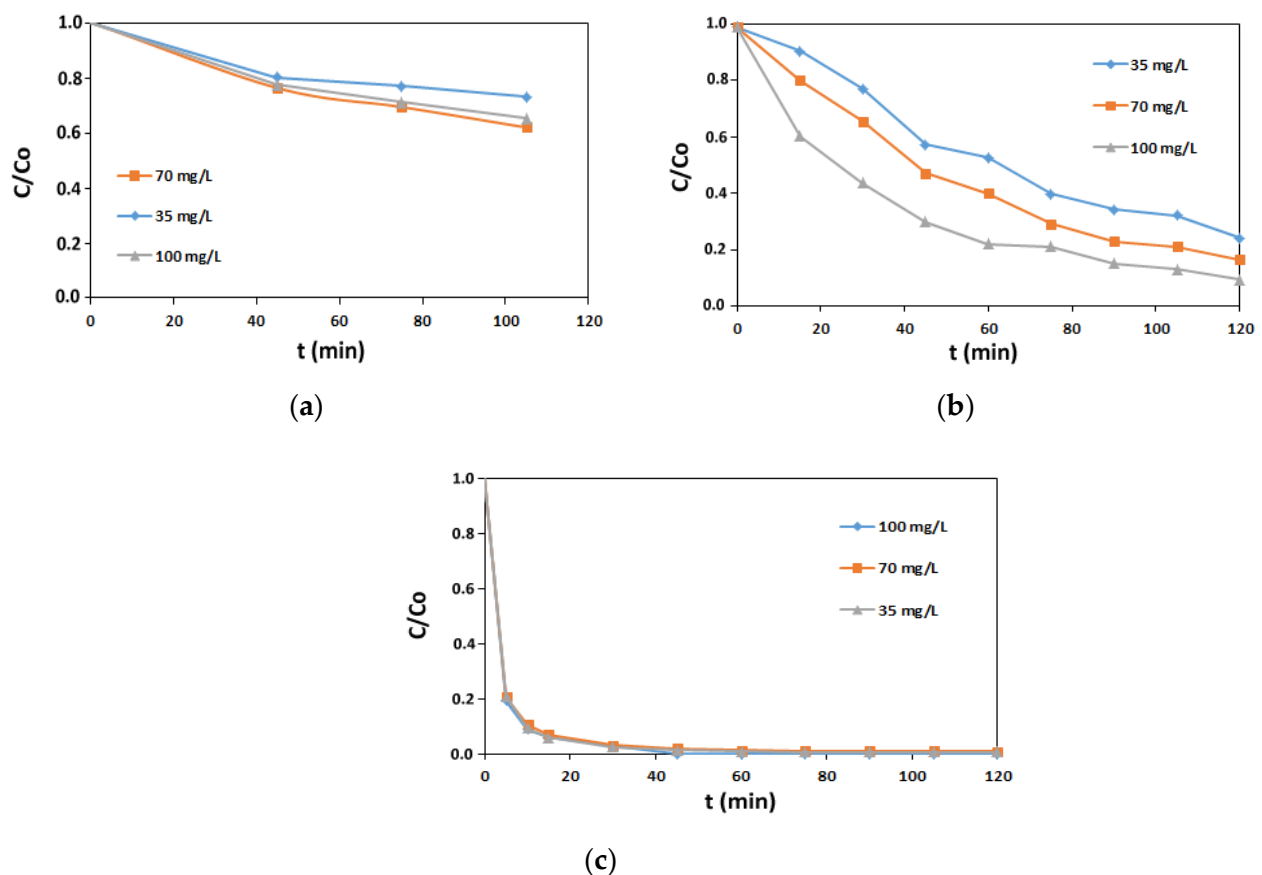
Figure 6. Effect of (**a**) H_2O_2 alone, (**b**) H_2O_2 activated by simulated solar light and (**c**) H_2O_2 activated by Fe^{2+} ions on the concentration of AV1, calculated from the absorbance changes.

The experiments with hydrogen peroxide alone and with hydrogen peroxide activated by simulated solar radiation were conducted at a pH of 9, which, according to the literature, is optimal for the oxidation process [59]. The Fenton processes were conducted at a pH of 3, which provides the highest oxidation efficiency and prevents the removal of Fe^{2+} ions by precipitation as $Fe(OH)_2$ [60]. To determine the influence of the amount of oxidant on the course of the process, tests were carried out for three concentrations of H_2O_2: 35, 70 and 100 mg/L. The data presented in Figure 6 indicate that, under the action of H_2O_2, there is a slight decrease in the concentration of AV1, and C/C_0 take values between 0.65 and 0.73, depending on the concentration of the oxidant. In the case of H_2O_2 activated by simulated solar radiation, after 120 min of oxidation, C/C_0 equals 0.09 and 0.24, which means that 9% to 24% of the original dye concentration remains in the system. As a result of the Fenton process, after 15 min, the C/C_0 of AV1 in the system decrease to 0.06–0.07. After 45–60 min of oxidation in the H_2O_2/Fe^{2+} system, the concentration of AV1 decreases to values undetectable by the spectrophotometric method. The concentration of the oxidant is an important factor in the effectiveness of the oxidation process. When the initial H_2O_2 concentration is growing, the degradation rate of AV1 increases (Figure 6a–c). This is associated with an increase in the concentration of reactive $^\cdot OH$ radicals along with a greater concentration of H_2O_2. The greatest differences in the course of UV1 degradation processes in the presence of different concentrations of hydrogen peroxide were observed for the $H_2O_2/$sunlight system. In this system, after 120 min of oxidation, the C/C_0 values were 0.24, 0.16 and 0.9 when the oxidant concentration was 35, 70 and 100 mg/L, respectively.

Concentration data plotted against time on a semi-log scale form straight lines (Figure 7), which indicates that the all oxidation processes based on the use of H_2O_2 follow pseudo-first-order kinetics. The slope of the corresponding line equals the rate constant (k_1), according to Equation (15):

$$\ln\left(\frac{C}{C_0}\right) = -k_1 t \tag{15}$$
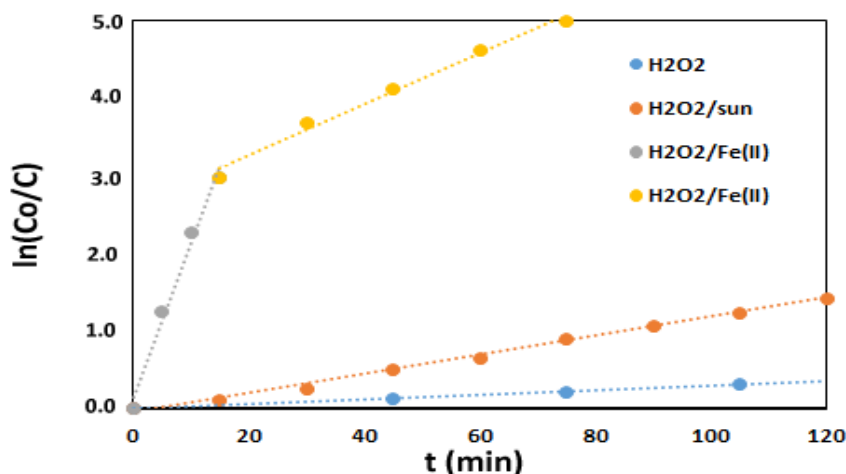
Figure 7. Semi-log plots for AV1 concentration decay in the presence of H_2O_2 alone, $H_2O_2/$sunlight, H_2O_2/Fe^{2+} ($C_{H_2O_2}$ = 35 mg/L).

Therefore, the half-life of AV1 in the considered oxidation systems can be calculated from the following relationship:

$$t_{1/2} = -\frac{\ln 0.5}{k_1} \tag{16}$$

The time required to remove 99% of the original amount of dye can be calculated from the following formula:

$$t_{99\%} = -\frac{\ln 0.01}{k_1} \tag{17}$$

As could be seen in Figure 7, in the case of the H_2O_2 alone and H_2O_2/sunlight systems, one equation describes the rate of oxidation over the entire time range. However, when we consider Fenton's reaction, it could be seen that the process starts at a higher speed, and then the speed is decreased. In this case, the kinetic diagram can be divided into two areas in which the linear course of the function $\ln(C_0/C)$ is described by different equations. The values of the determination coefficient describing the fit of the experimental data to the theoretical course of the function, as well as k_1 and $t_{1/2}$ values for AV1 degradation, are included in Table 5.

Table 5. Determination coefficients (R^2) describing the fit of the experimental data to the theoretical course of the $\ln(C/C_0) = f(t)$ function, first-order rate constant (k_1), half-life time ($t_{1/2}$) and time required to achieve 99% ($t_{99\%}$) AV1 removal by H_2O_2 ($C_{H_2O_2}$ = 35 mg/L)-based oxidation.

Degradation Process	R^2	k_1 (min^{-1})	$t_{1/2}$ (min)	$t_{99\%}$ (min)
H_2O_2 alone	0.999	0.0030	231	1535
H_2O_2/sunlight	0.999	0.0123	56	374
Fenton (0–15 min)	0.993	0.2001	3.5	23
Fenton (15–75 min)	0.994	0.0330	21	140

As can be seen in Table 4, the removal of AV1 by oxidation with H_2O_2 is a relatively lengthy process. It occurs most quickly in the Fenton system. Similar results are obtained in studies on the removal of other azo dyes [35]. Zuorro and Lavecchia, in their work on the removal of Reactive Green 19, obtained a shorter dye removal time when H_2O_2 was assisted by UV radiation [36]. However, such a system consumes large amounts of energy, while the use of sunlight is a cheaper and more environmentally friendly solution.

3.2.2. PAA Based Oxidation

So far, the use of PAA as an oxidant in AOPs has been relatively little researched, and only single studies concern its use for the removal of organic compounds from water and wastewater [41]. For over a dozen years, PAA has been considered to be a very efficient disinfectant. Currently, it is increasingly used for the final sterilization of treated wastewater [42,61]. Peracetic acid undergoes slow autodecomposition (7.36×10^{-3} 1/M·s) at room temperature [41]. Due to its high oxidation potential, it is able to react with organic micropollutants present in water. Under the influence of light, the O–O bond in PAA decomposes, which leads to the formation of HO$^{\bullet}$ and acetyloxyl radicals ($CH_3C(O)O^{\bullet}$):

$$CH_3C(O)OOH + h\nu \rightarrow HO^{\bullet} + CH_3C(O)O^{\bullet} \tag{18}$$

PAA can also be activated with Fe^{2+}, analogous to H_2O_2 in the Fenton process:

$$CH_3C(O)OOH + Fe^{2+} \rightarrow CH3C(O)O^{\bullet} + OH^- + Fe^{3+} \tag{19}$$

$$CH_3C(O)OOH + Fe^{2+} \rightarrow CH3C(O)O^- + OH^{\bullet} + Fe^{3+} \tag{20}$$

$$CH_3C(O)OOH + Fe^{2+} \rightarrow CH3C(O)OH + Fe^{IV}O^{2+} \tag{21}$$

The formed radicals can react with PAA, acetic acid and H_2O_2 to form secondary radicals—among others, superoxide radical anion ($O_2-^{\bullet}$), hydroperoxyl radical (HO$_2^{\bullet}$) and methyl radical ($^{\bullet}CH_3$). Since H_2O_2 is also present in the PAA solution, the reactions described by Equations (6)–(8) may also take place during the oxidation. However, the literature data show that these processes are characterized by a much slower speed than those involving PAA [58].

Experiments with peracetic acid were conducted at a pH of 7 when the oxidant was used alone and when the oxidant was activated by solar radiation. A pH of 3 was chosen as optimal for systems in which PAA was activated with iron ions [41]. Figure 8 shows the effect of contact with PAA alone, PAA/sunlight, PAA/Fe^{2+} and PAA/Fe^{2+}/sunlight on the concentration of AV1, calculated from the absorbance changes. The research was carried

out for three PAA concentrations (35, 70, 100 mg/L) in the case of the first two experiments. The data presented in Figure 8a indicate that PAA alone causes very little decolorization of AV1. The C/C_0 value after 120 min of the experiment decreased to 0.75–0.82. In the PAA/sunlight system (Figure 8b), the dye content after 120 min of the experiment decreased to 29–42% of the initial concentration. In the case of PAA alone and PAA activated by sunlight, the degree of degradation increases with the increase in the concentration of the oxidant, which is related to the greater number of radicals formed during the processes. The differences in the degree of AV1 removal in the solutions with the highest and the lowest oxidant concentration range from a few to a dozen percentage points. The experiments in PAA/Fe^{2+} and PAA/Fe^{2+}/sunlight systems were performed for five concentrations of the oxidant: 12.5, 35, 50, 70 and 100 mg/L (Figure 8c,d). In the first of these systems, the C/C_0 of AV1 achieves values from 0 to 0.08 after 120 min of oxidation. In total, 5% of the initial AV1 concentration remains after 5 min of oxidation in solutions where the concentration of the PAA is 12.5 or 35 mg/L. When the oxidant concentration is 50 and 70 mg/L, 95% degradation is achieved after 75 and 90 min of the experiment, respectively. At an oxidant concentration of 100 mg/L, this degree of degradation is not achieved within the 120 min of the experiment. In the PAA system, the concentration of AV1 is reduced to a level from 0% to 2% of the initial value within 120 min. AV1 solution discoloration at the level of 95% occurs after 5 min of contact with the oxidant, when the concentration of PAA is 12.5 or 35 mg/L and after 15 min, when C_{PAA} is 50 or 70 mg/L. With a C_{PAA} of 100 mg/L, 95% decolorization occurs within 60 min. We found that 35 mg/L is the optimal oxidant concentration for the most efficient dye removal in PAA/Fe^{2+} and PAA/Fe^{2+}/sunlight systems. Only slightly worse results are achieved when the concentration is 12.5 mg/L. Fe^{2+} ions activate PAA and the H$_2$O$_2$ in equilibrium with it, causing the intensive production of radicals with high oxidizing potential. These radicals react and quench each other, which lowers the oxidizing potential of the system.

As can be seen in Figure 9, all oxidation processes with the use of PAA proceed according to the pseudo-first-order kinetics. The correlation coefficients for all considered processes are 0.99 or more, which indicates a very good fit of the experimental data to the theoretical course of the function $\ln(C/C_0) = f(t)$. Table 6 shows the values of R^2, k_1, $t_{1/2}$ and $t_{99\%}$ for PAA-based AV1 degradation. The dye removal is very fast in PAA/Fe^{2+}/sunlight ($k_1 = 0.3897$ min^{-1}) and PAA/Fe^{2+} ($k_1 = 0.3527$ min^{-1}) systems, and after 15 min, the solution is completely discolored. The processes in the PAA and PAA/sunlight systems run at a low speed, the constant rates are 0.0017 and 0.0070 min^{-1}, respectively.

(**a**)

(**b**)

Figure 8. *Cont.*

(**c**)

(**d**)
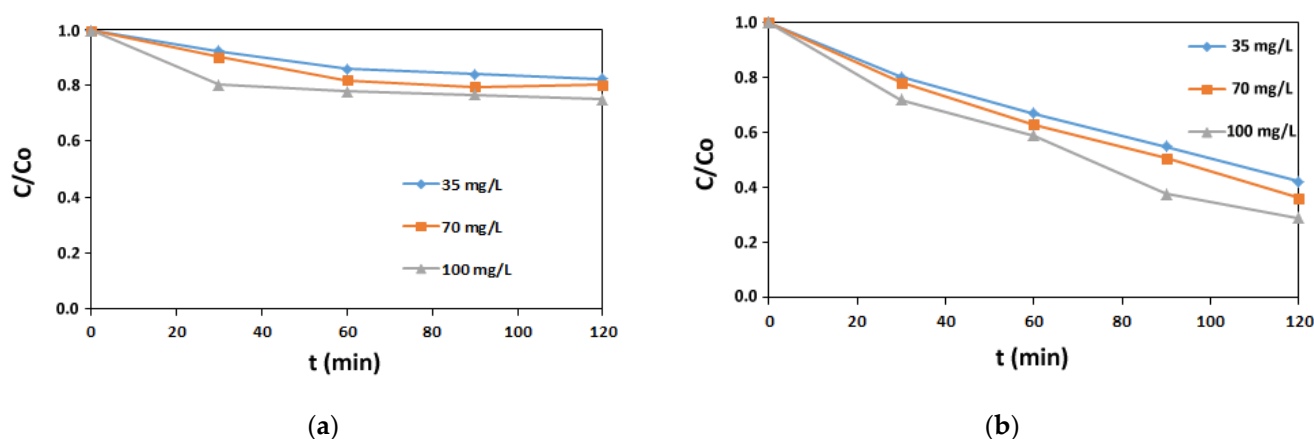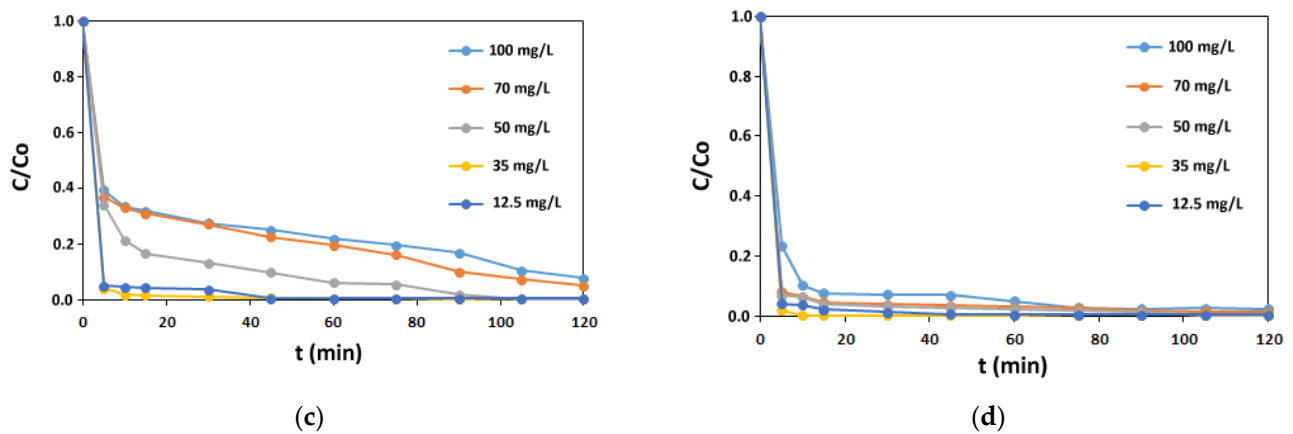
Figure 8. Effect of (**a**) PAA alone, (**b**) PAA activated by simulated solar light, (**c**) PAA activated by Fe^{2+} ions and (**d**) PAA activated by Fe^{2+} ions and solar light on the concentration of AV1, calculated from the absorbance changes.
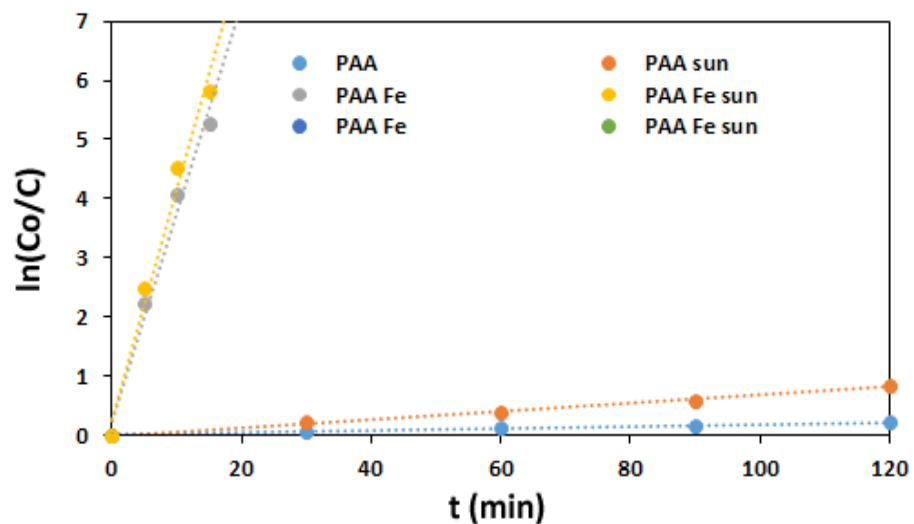
Figure 9. Semi-log plots for AV1 concentration decay in the presence of PAA alone, PAA/sunlight, PAA/Fe^{2+} and PAA/Fe^{2+}/sunlight (C_{PAA} = 35 mg/L).

Table 6. Determination coefficient (R^2) describing the fit of the experimental data to the theoretical course of the $\ln(C/C_0) = f(t)$ function, first-order rate constant (k_1), half-life time ($t_{1/2}$) and time required to achieve 99% ($t_{99\%}$) AV1 removal by PAA (C_{PAA} = 35 mg/L) based oxidation.

Degradation Proces	R^2	k_1 (min^{-1})	$t_{1/2}$ (min)	$t_{99\%}$(min)
PAA alone	0.990	0.0017	408	2709
PAA/sunlight	0.999	0.0070	99	658
PAA/Fe^{2+} (0–15 min)	0.991	0.3527	2	13
PAA/Fe^{2+}/sun (0–15 min)	0.991	0.3897	1.8	12

3.2.3. AV1 Removal Efficiency in Oxidation Processes

The efficiency of AV1 removal in oxidation processes was determined both on the basis of the degree of decolorization and on the basis of changes in the COD value (Figure 10). The COD value determined by the potassium dichromate(VI) method is 145 mg O_2/L for the 100 mg/L AV1 solution, which was used in all oxidation experiments. The comparison of the efficiency of oxidation processes based on the use of H_2O_2 and PAA shows that the best oxidation results are provided by systems in which the oxidant is activated with iron ions.

(a)

(b)
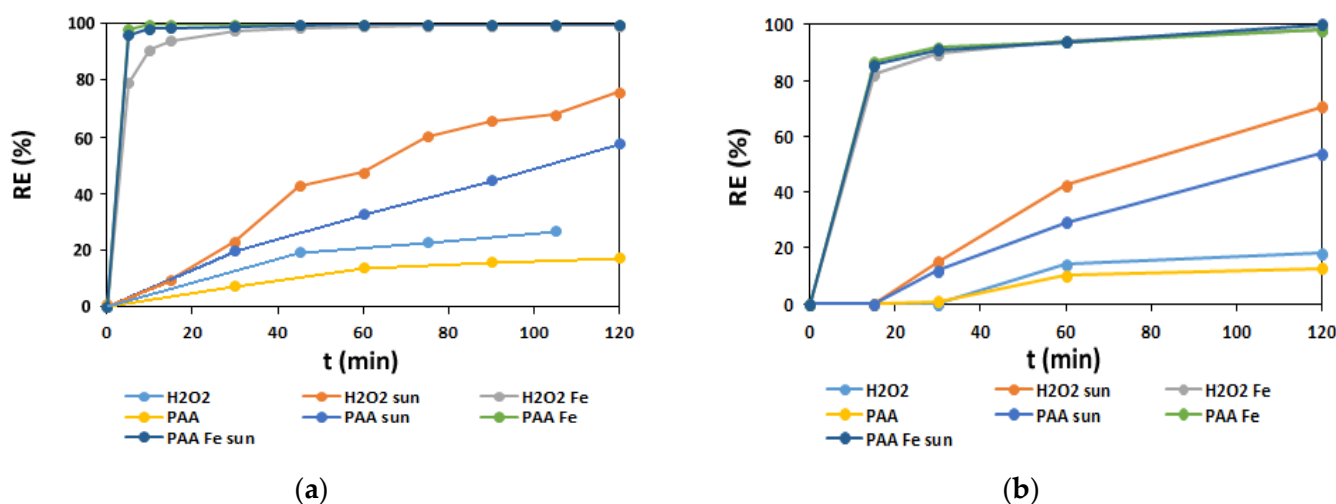
Figure 10. Removal efficiency of AV1 in different oxidation systems, measured as (**a**) decolorization and (**b**) mineralization ratio ($C_{H_2O_2} = C_{PAA} = 35$ mg/L).

As shown in Figure 10a, the decolorization efficiency in systems with PAA and Fe^{2+} ions takes values close to 100% in a shorter time than in the H_2O_2/Fe^{2+} system. This is probably related to the higher oxidation potential (E_0); i.e., PAA: $E_0 = 1.96V$; H_2O_2: $E_0 = 1.78$ V [42]. The higher efficiency of PAA oxidation is probably also influenced by the fact that the oxygen–oxygen bond energy for this compound is lower (170 kJ/mol) than for H_2O_2 (210 kJ/mol). Furthermore, the peroxy bond in the PAA molecule is longer than in H_2O_2 (1.443 Å and 1.427 Å, respectively), so it is easily broken, leading to the formation of hydroxyl and acetate radicals [41]. The COD reduction efficiency presented in Figure 10b is related to the gradual mineralization of AV1; i.e., its degradation to inorganic ions. As can be seen, the mineralization of the oxidized solution takes place slower than its decolorization. The obtained results are consistent with literature reports; similar observations were made for the oxidation of Erythrosine B, Orange G and Reactive Green 19 by H_2O_2/UV, photo-Fenton, electro-Fenton, UV-electro-Fenton and solar-electro-Fenton processes [36,37,40]. After 120 min of oxidation, almost complete mineralization of the solution takes place in all systems where Fe^{2+} ions are present. The confirmation of complete mineralization is very important as it confirms the degradation of AV1 to simple inorganic ions and not to potentially toxic, and at the same time colorless, intermediates [36].

4. Conclusions

This paper describes the results of C.I. Acid Violet 1 (azo class dye) removal from aqueous solutions and dyeing baths using two techniques—adsorption and advanced oxidation—taking into consideration different experimental conditions. In adsorption tests, the selectivity of the macroporous strongly basic anion exchangers (Purolite A520E and Lewatit S5428) with quaternary ammonium functional groups differing in the chemical composition of the matrix was evaluated. Large values of the sorption capacities of both resins described by the Langmuire and Freundlich isotherm model allowed their use in the removal of AV1 dye, also in the presence of salts and surfactants. The dye removal efficiency reached more than 99% after 240 min in 100–500 mg/L solutions using A520E and S5428. The effective regeneration of the adsorbents has also been proposed, which enables their practical application.

The results of oxidation experiments indicate that AOPs based on H_2O_2 and PAA can effectively remove AV1 from its water solutions. Both sunlight and iron ions used as oxidation activators accelerate the degradation of the tested dye. The Fenton reaction, PAA/Fe^{2+} and PAA/Fe^{2+}/sunlight systems are most effective in both the decolorization and mineralization of AV1 solutions. It was found that PAA, which is an oxidant that is rarely used and relatively little studied, works more efficiently and faster than H_2O_2. In

addition, oxidation with PAA requires lower concentrations of the oxidant than in the case of H_2O_2, which reduces the cost of the process and the impact on the environment.

In conclusion, the proposed techniques can be considered as highly effective for the removal of AV1, and the performed studies are of significant importance not only from a scientific but also from a practical point of view, especially in the treatment of wastewaters containing acid-type dyes.

Author Contributions: Conceptualization, M.W. and U.K.; methodology, M.W. and U.K.; validation, M.W., U.K. and A.S.; investigation, M.W., U.K. and A.S.; resources, M.W., U.K. and A.S.; data curation, M.W., U.K. and A.S.; writing—original draft preparation, M.W. and U.K.; writing—review and editing, M.W. and U.K.; visualization, M.W. and U.K.; supervision, M.W. and U.K. All authors have read and agreed to the published version of the manuscript.

Data Availability Statement: The data presented in this study are available in this article.

References

1. Sen, T.K.; Afroze, S.; Ang, H. Equilibrium, kinetics and mechanism of removal of methylene blue from aqueous solution by adsorption onto pine cone biomass of Pinus radiata. *Water Air Soil Pollut.* **2011**, *218*, 499–515. [CrossRef]
2. Yagub, M.T.; Sen, T.K.; Ang, H. Equilibrium, kinetics, and thermodynamics of methylene blue adsorption by pine tree leaves. *Water Air Soil Pollut.* **2012**, *223*, 5267–5282. [CrossRef]
3. Banat, I.M.; Nigam, P.; Singh, D.; Marchant, R. Microbial decolorization of textile-dye containing effluents: A review. *Bioresour. Technol.* **1996**, *58*, 217–227. [CrossRef]
4. Mittal, A.K.; Gupta, S. Biosorption of cationic dyes by dead macro fungus Fomitopsis carnea: Batch studies. *Water Sci. Technol.* **1996**, *34*, 81–87. [CrossRef]
5. Fu, Y.; Viraraghavan, T. Fungal decolorization of dye wastewaters: A review. *Bioresour. Technol.* **2001**, *79*, 251–262. [CrossRef]
6. Mishra, G.; Tripathy, M.A. critical review of the treatments for decolourization of textile effluent. *Colourage* **1993**, *40*, 35–45.
7. Lazar, T. Color chemistry: Synthesis, properties, and applications of organic dyes and pigments. *Color. Res. Appl.* **2005**, *30*, 313–314. [CrossRef]
8. Robinson, T.; McMullan, G.; Marchant, R.; Nigam, P. Remediation of dyes in textile effluent: A critical review on current treatment technologies with a proposed alternative. *Bioresour. Technol.* **2001**, *77*, 247–255. [CrossRef]
9. Tkaczyk, A.; Mitrowska, K.; Posyniak, A. Synthetic organic dyes as contaminants of the aquatic environment and their implications for ecosystems: A review. *Sci. Total Environ.* **2020**, *717*, 137222. [CrossRef]
10. Kadirvelu, K.; Kavipriya, M.; Karthika, C.; Radhika, M.; Vennilamani, N.; Pattabhi, S. Utilization of various agricultural wastes for activated carbon preparation and application for the removal of dyes and metal ions from aqueous solutions. *Bioresour. Technol.* **2003**, *87*, 129–132. [CrossRef]
11. Ishak, S.A.; Murshed, M.F.; Md Akil, H.; Ismail, N.; Md Rasib, S.Z.; Al-Gheethi, A.A.S. The application of modified natural polymers in toxicant dye compounds wastewater: A review. *Water* **2020**, *12*, 2032. [CrossRef]
12. Argumedo-Delira, R.; Gómez-Martínez, M.J.; Uribe-Kaffure, R. Trichoderma biomass as an alternative for removal of congo red and malachite green industrial dyes. *Appl. Sci.* **2021**, *11*, 448. [CrossRef]
13. Duhan, M.; Kaur, R. Nano-structured polyaniline as a potential adsorbent for methylene blue dye removal from effluent. *J. Compos. Sci.* **2021**, *5*, 7. [CrossRef]
14. Ma, C.M.; Hong, G.B.; Wang, Y.K. Performance evaluation and optimization of dyes removal using rice bran-based magnetic composite adsorbent. *Materials* **2020**, *13*, 2764. [CrossRef] [PubMed]
15. Ghoreishi, S.; Haghighi, R. Chemical catalytic reaction and biological oxidation for treatment of non-biodegradable textile effluent. *Chem. Eng. J.* **2003**, *95*, 163–169. [CrossRef]
16. Yagub, M.T.; Kanti Sen, T.; Afroze, S.; Ang, H.M. Dye and its removal from aqueous solution by adsorption: A review. *Adv. Colloid Interface Sci.* **2014**, *209*, 172–184. [CrossRef]
17. Kant, R. Adsorption of dye eosin from an aqueous solution on two different samples of activated carbon by static batch method. *J. Water Resour. Prot.* **2012**, *4*, 93–98. [CrossRef]
18. Seifikar, F.; Azizian, S.; Sillanpää, M. Microwave-assisted synthesis of carbon powder for rapid dye removal. *Mater. Chem. Phys.* **2020**, *250*, 123057. [CrossRef]

19. Rehman, M.S.U.; Kim, I.; Han, J.I. Adsorption of methylene blue dye from aqueous solution by sugar extracted spent rice biomass. *Carbohydr. Polym.* **2012**, *90*, 1314–1322. [CrossRef]
20. Zhang, W.-X.; Laia, L.; Meia, P.; Lia, Y.; Lia, Y.-H.; Liu, Y. Enhanced removal efficiency of acid red 18 from aqueous solution using wheat bran modified by multiple quaternary ammonium salts. *Chem. Phys. Lett.* **2018**, *710*, 193–201. [CrossRef]
21. Gupta, V. Application of low-cost adsorbents for dye removal-a review. *J. Environ. Manag.* **2009**, *90*, 2313–2342. [CrossRef]
22. Karcher, S.; Kornmüller, A.; Jekel, M. Anion exchange resins for removal of reactive dyes from textile wastewaters. *Water Res.* **2002**, *36*, 4717–4724. [CrossRef]
23. Wawrzkiewicz, M.; Hubicki, Z. Remazol Black B removal from aqueous solutions and wastewater using weakly basic anion exchange resins. *Cent. Eur. J. Chem.* **2011**, *9*, 867–876. [CrossRef]
24. Wawrzkiewicz, M. Comparison of gel anion exchangers of various basicity in direct dye removal from aqueous solutions and wastewaters. *Chem. Eng. J.* **2011**, *173*, 773–781. [CrossRef]
25. Wawrzkiewicz, M. Anion exchange resins as effective sorbents for acidic dye removal from aqueous solutions and wastewaters. *Solvent Extr. Ion Exch.* **2012**, *30*, 507–523. [CrossRef]
26. Wawrzkiewicz, M. Comparison of the efficiency of Amberlite IRA 478RF for acid, reactive, and direct dyes removal from aqueous media and wastewaters. *Ind. Eng. Chem. Res.* **2012**, *51*, 8069–8078. [CrossRef]
27. Wawrzkiewicz, M. Anion-exchange resins for C.I. Direct Blue 71 removal from aqueous solutions and wastewaters: Effects of basicity and matrix composition and structure. *Ind. Eng. Chem. Res.* **2014**, *53*, 11838–11849. [CrossRef]
28. Kaušpėdienė, D.; Gefenienė, A.; Kazlauskienė, E.; Ragauskas, R.; Selskienė, A. Simultaneous removal of azo and phthalocyanine dyes from aqueous solutions using weak base anion exchange resin. *Water Air Soil Pollut.* **2013**, *224*, 1769–1781. [CrossRef]
29. Polska-Adach, E.; Wawrzkiewicz, M. Removal of acid, direct and reactive dyes on the polyacrylic anion exchanger. *Physicochem. Probl. Miner. Process.* **2019**, *55*, 1496–1508. [CrossRef]
30. Wawrzkiewicz, M.; Polska-Adach, E. Physicochemical interactions in systems C.I. Direct Yellow 50—weakly basic resins: Kinetic, equilibrium, and auxiliaries addition aspects. *Water* **2021**, *13*, 385. [CrossRef]
31. Wawrzkiewicz, M.; Podkościelna, B.; Podkościelny, P. Application of functionalized DVB-*co*-GMA polymeric microspheres in the enhanced sorption process of hazardous dyes from dyeing baths. *Molecules* **2020**, *25*, 5247. [CrossRef] [PubMed]
32. Ma, D.; Yi, H.; Lai, C.; Liu, X.; Huo, X.; An, Z.; Li, L.; Fu, Y.; Li, B.; Zhang, M.; et al. Critical review of advanced oxidation processes in organic wastewater treatment. *Chemosphere* **2021**, *275*, 130104. [CrossRef]
33. Ikehata, K.; Gamal El-Din, M. Aqueous pesticide degradation by hydrogen peroxide/ultraviolet irradiation and Fenton-type advanced oxidation processes: A review. *J. Environ. Eng. Sci.* **2006**, *5*, 81–135. [CrossRef]
34. Boczkaj, G.; Fernandes, A. Wastewater treatment by means of advanced oxidation processes at basic pH conditions: A review. *Chem. Eng. J.* **2017**, *320*, 608–633. [CrossRef]
35. Corona-Bautista, M.; Picos-Benítez, A.; Villaseñor-Basulto, D.; Bandala, E.; Peralta-Hernández, J.M. Discoloration of azo dye Brown HT using different advanced oxidation processes. *Chemosphere* **2021**, *267*, 129234. [CrossRef]
36. Zuorro, A.; Lavecchia, R. Evaluation of UV/H_2O_2 advanced oxidation process (AOP) for the degradation of diazo dye Reactive Green 19 in aqueous solution. *Desalin. Water Treat.* **2014**, *52*, 1571–1577. [CrossRef]
37. Tarkwa, J.B.; Oturan, N.; Acayanka, E.; Laminsi, S.; Oturan, M.A. Photo-Fenton oxidation of Orange G azo dye: Process optimization and mineralization mechanism. *Environ. Chem. Lett.* **2019**, *17*, 473–479. [CrossRef]
38. Oliveira, M.; Neves, N.; Santana, R.; Lucena, A.; Zaidan, L.; Cavalcanti, V.; Silva, G.; Napoleão, D. Employment of advanced oxidation processes in the degradation of a textile dye mixture: Evaluation of reaction parameters, kinetic study, toxicity and modeling by artificial neural networks. *REGET* **2021**, *25*, 12. [CrossRef]
39. Çiner, F.; Gökkuş, Ö. Treatability of dye solutions containing disperse dyes by Fenton and Fenton-solar light oxidation processes. *Clean-Soil Air Water* **2013**, *41*, 80–85. [CrossRef]
40. Clematis, D.; Panizza, M. Electro-Fenton, solar photoelectro-Fenton and UVA photoelectro-Fenton: Degradation of Erythrosine B dye solution. *Chemosphere* **2021**, *270*, 129480. [CrossRef]
41. Kiejza, D.; Kotowska, U.; Polińska, W.; Karpińska, J. Peracids—New oxidants in advanced oxidation processes: The use of peracetic acid, peroxymonosulfate, and persulfate salts in the removal of organic micropollutants of emerging concern—A review. *Sci. Total Environ.* **2021**, *790*, 148195. [CrossRef] [PubMed]
42. Ao, X.-W.; Eloranta, J.; Huang, C.-H.; Santoro, D.; Sun, W.-J.; Lu, Z.-D.; Li, C. Peracetic acid-based advanced oxidation processes for decontamination and disinfection of water: A review. *Water Res.* **2021**, *188*, 116479. [CrossRef]
43. Ghanbari, F.; Moradi, M. Application of peroxymonosulfate and its activation methods for degradation of environmental organic pollutants: Review. *Chem. Eng. J.* **2017**, *310*, 41–62. [CrossRef]
44. Babu, D.S.; Srivastava, V.; Nidheesh, P.V.; Kumar, M.S. Detoxification of water and wastewater by advanced oxidation processes. *Sci. Total Environ.* **2019**, *696*, 133961. [CrossRef]
45. Available online: https://www.purolite.com/product-pdf/A520E.pdf (accessed on 23 February 2021).
46. Available online: https://www.lenntech.com/Data-sheets/Lewatit-S-5428-L.pdf (accessed on 23 February 2021).
47. Langmuir, I. The adsorption of gases on plane surfaces of glass, mica and platinum. *J. Am. Chem. Soc.* **1918**, *40*, 1361–1403. [CrossRef]
48. Freundlich, H.M.F. Over the adsorption in solution. *J. Phys. Chem.* **1906**, *57*, 385–470. [CrossRef]
49. Tempkin, M.I.; Pyzhev, V. Kinetics of ammonia synthesis on promoted iron catalyst. *Acta Physicochim. USSR* **1940**, *12*, 327–356.

50. Bulut, E.; Özacar, M.; Şengil, İ.A. Equilibrium and kinetic data and process design for adsorption of Congo Red onto bentonite. *J. Hazard. Mater.* **2008**, *154*, 613–622. [CrossRef] [PubMed]
51. Webber, T.W.; Chakkravorti, R.K. Pore and solid diffusion models for fixed-bed adsorbers. *AlChE J.* **1974**, *20*, 228–238. [CrossRef]
52. Namasivayam, C.; Yamuna, R.; Arasi, D.J.S.E. Removal of acid violet from wastewater by adsorption on waste red mud. *Environ. Geol.* **2001**, *41*, 269–273. [CrossRef]
53. Krysztafkiewicz, A.; Binkowski, S.; Jesionowski, T. Adsorption of dyes on a silica surface. *Appl. Surf. Sci.* **2002**, *199*, 31–39. [CrossRef]
54. Wrzesińska, K.; Wawrzkiewicz, M.; Szymczyk, K. Physicochemical interactions in C.I. Acid Green 16–Lewatit S 6368A systems–kinetic, equilibrium, auxiliaries addition and thermodynamic aspects. *J. Mol. Liq.* **2021**, *331*, 115748. [CrossRef]
55. Kotowska, U.; Wawrzkiewicz, M.; Polska-Adach, E. Mechanism of interactions in C.I. Acid Red 18–Floating plants and polymeric resins systems: Kinetic, equilibrium, auxiliaries impact and column studies. *J. Mol. Liq.* **2021**, *333*, 115903. [CrossRef]
56. Kuznetsov, M.L.; Teixeira, F.A.; Bokach, N.A.; Pombeiro, A.J.L.; Shul'pin, G.B. Radical decomposition of hydrogen peroxide catalyzed by aqua complexes $[M(H_2O)_n]^{2+}$ (M=Be, Zn, Cd). *J. Catal.* **2014**, *313*, 135–148. [CrossRef]
57. He, J.; Yang, X.; Men, B.; Wang, D. Interfacial mechanisms of heterogeneous Fenton reactions catalyzed by iron-based materials: A review. *J. Environ. Sci.* **2016**, *39*, 97–109. [CrossRef]
58. Kim, J.; Zhang, T.; Liu, W.; Du, P.; Dobson, J.T.; Huang, C.-H. Advanced oxidation process with peracetic acid and Fe(II) for contaminant degradation. *Environ. Sci. Technol.* **2019**, *53*, 13312–13322. [CrossRef]
59. Tosik, R. Dyes color removal by ozone and hydrogen peroxide: Some aspects and problems. *Ozone Sci. Eng.* **2005**, *27*, 265–271. [CrossRef]
60. Rehman, F.; Sayed, M.; Khan, J.A.; Shah, L.A.; Shah, N.S.; Khan, H.M.; Khattak, R. Degradation of Crystal Violet dye by Fenton and photo-Fenton oxidation processes. *Z. Für Phys. Chem.* **2018**, *232*, 1771–1786. [CrossRef]
61. Rokhina, E.; Makarova, K.; Lahtinen, M.; Golovina, E.; As, H.; Virkutyte, J. Ultrasound-assisted MnO_2 catalyzed homolysis of peracetic acid for phenol degradation: The assessment of process chemistry and kinetics. *Chem. Eng. J.* **2013**, *221*, 476–486. [CrossRef]